FMT gave the high-contrast image of the tumor due to the low background. The utility of D-[^{18}F]FMT was especially demonstrated in the orthotopic brain tumor model. Thus D-[^{18}F]FMT appears promising as a tumor-detecting agent for PET diagnosis.

Acknowledgments

We gratefully acknowledge Mr. Kengo Sato and Mr. Norihiro Harada (Hamamatsu Photonics K.K.) for the synthesis of D- and L-isomers of [^{18}F]FMT.

References

[1] Kubota R, Kubota K, Yamada S, Tada M, Ido T, Tamahashi N. Microautoradiographic study for the differentiation of intratumoral macrophages, granulation tissues and cancer cells by the dynamics of fluorine-18-fluorodeoxyglucose uptake. J Nucl Med 1994;35:104–12.

[2] Ishiwata K, Vaalburg W, Elsinga PH, Paans AM, Woldring MG. Comparison of L-[1-^{11}C]methionine and L-methyl-[^{11}C]methionine for measuring in vivo protein synthesis rates with PET. J Nucl Med 1988; 29:1419–27.

[3] Comar D, Cartron J, Maziere M, Marazano C. Labelling and metabolism of methionine-methyl-^{11}C. Eur J Nucl Med 1976;1:11–4.

[4] Ishiwata K, Vaalburg W, Elsinga PH, Paans AM, Woldring MG. Metabolic studies with L-[1-^{14}C]tyrosine for the investigation of a kinetic model to measure protein synthesis rates with PET. J Nucl Med 1988;29:524–9.

[5] Barrio JR, Keen RE, Ropchan JR, MacDonald NS, Baumgartner FJ, Padgett HC, et al. L-[1-^{11}C]leucine: routine synthesis by enzymatic resolution. J Nucl Med 1983;24:515–21.

[6] Casey DL, Digenis GA, Wesner DA, Washburn LC, Chaney JE, Hayes RL, et al. Preparation and preliminary tissue studies of optically active ^{11}C-D- and L-phenylalanine. Int J Appl Radiat Isot 1981;32:325–30.

[7] Lemaire C, Guillaume M, Christiaens L, Palmer AJ, Cantineau R. A new route for the synthesis of [^{18}F]fluoroaromatic substituted amino acids: no carrier added L-*p*-[^{18}F]fluorophenylalanine. Int J Rad Appl Instrum [A] 1987;38:1033–8.

[8] Coenen HH, Kling P, Stocklin G. Cerebral metabolism of L-[2-^{18}F] fluorotyrosine, a new PET tracer of protein synthesis. J Nucl Med 1989;30:1367–72.

[9] Ishiwata K, Kawamura K, Wang WF, Furumoto S, Kubota K, Pascali C, et al. Evaluation of *O*-[^{11}C]methyl-L-tyrosine and *O*-[^{18}F]fluoromethyl-L-tyrosine as tumor imaging tracers by PET. Nucl Med Biol 2004;31:191–8.

[10] Wester HJ, Herz M, Weber W, Heiss P, Senekowitsch-Schmidtke R, Schwaiger M, et al. Synthesis and radiopharmacology of *O*-(2-[^{18}F] fluoroethyl)-L-tyrosine for tumor imaging. J Nucl Med 1999;40:205–12.

[11] Heiss P, Mayer S, Herz M, Wester HJ, Schwaiger M, Senekowitsch-Schmidtke R. Investigation of transport mechanism and uptake kinetics of *O*-(2-[^{18}F]fluoroethyl)-L-tyrosine in vitro and in vivo. J Nucl Med 1999;40:1367–73.

[12] Tang G, Tang X, Wang M, Luo L, Gan M. Fully automated synthesis of *O*-(3-[^{18}F]fluoropropyl)-L-tyrosine by direct nucleophilic exchange on a quaternary 4-aminopyridinium resin. Appl Radiat Isot 2003;58: 685–9.

[13] Tang G, Wang M, Tang X, Luo L, Gan M. Synthesis and evaluation of *O*-(3-[^{18}F]fluoropropyl)-L-tyrosine as an oncologic PET tracer. Nucl Med Biol 2003;30:733–9.

[14] Ishiwata K, Kasahara C, Hatano K, Ishii S, Senda M. Carbon-11 labeled ethionine and propionine as tumor detecting agents. Ann Nucl Med 1997;11:115–22.

[15] Tamemasa O, Goto R, Takeda A, Maruo K. High uptake of ^{14}C-labeled D-amino acids by various tumors. Gann 1982;73:147–52.

[16] Takeda A, Goto R, Tamemasa O, Chaney JE, Digenis GA. Biological evaluation of radiolabeled D-methionine as a parent compound in potential nuclear imaging. Radioisotopes 1984;33:213–7.

[17] Goto R, Unno K, Takeda A, Okada S, Tamemasa O. Tumor accumulation of D-selenomethionine-75Se in tumor-bearing mice. J Pharmacobiodyn 1987;10:456–61.

[18] Martineau M, Baux G, Mothet JP. D-Serine signalling in the brain: friend and foe. Trends Neurosci 2006;29:481–91.

[19] Long Z, Sekine M, Adachi M, Furuchi T, Imai K, Nimura N, et al. Cell density inversely regulates D- and L-aspartate levels in rat pheochromocytoma MPT1 cells. Arch Biochem Biophys 2002;404: 92–7.

[20] Bendikov I, Nadri C, Amar S, Panizzutti R, De Miranda J, Wolosker H, et al. A CSF and postmortem brain study of D-serine metabolic parameters in schizophrenia. Schizophr Res 2007;90:41–51.

[21] Katsuki H, Nonaka M, Shirakawa H, Kume T, Akaike A. Endogenous D-serine is involved in induction of neuronal death by *N*-methyl-D-aspartate and simulated ischemia in rat cerebrocortical slices. J Pharmacol Exp Therapeut 2004;311:836–44.

[22] Homma H. Biochemistry of D-aspartate in mammalian cells. Amino Acids 2007;32:3–11.

[23] Kanai Y, Endou H. Heterodimeric amino acid transporters: molecular biology and pathological and pharmacological relevance. Curr Drug Metab 2001;2:339–54.

[24] Kanai Y, Segawa H, Miyamoto K, Uchino H, Takeda E, Endou H. Expression cloning and characterization of a transporter for large neutral amino acids activated by the heavy chain of 4F2 antigen (CD98). J Biol Chem 1998;273:23629–32.

[25] Segawa H, Fukasawa Y, Miyamoto K, Takeda E, Endou H, Kanai Y. Identification and functional characterization of a Na^+-independent neutral amino acid transporter with broad substrate selectivity. J Biol Chem 1999;274:19745–51.

[26] Nakamura E, Sato M, Yang H, Miyagawa F, Harasaki M, Tomita K, et al. 4F2 (CD98) heavy chain is associated covalently with an amino acid transporter and controls intracellular trafficking and membrane topology of 4F2 heterodimer. J Biol Chem 1999;274:3009–16.

[27] Kim DK, Kim IJ, Hwang S, Kook JH, Lee MC, Shin BA, et al. System L-amino acid transporters are differently expressed in rat astrocyte and C6 glioma cells. Neurosci Res 2004;50:437–46.

[28] Yanagida O, Kanai Y, Chairoungdua A, Kim DK, Segawa H, Nii T, et al. Human L-type amino acid transporter 1 (LAT1): characterization of function and expression in tumor cell lines. Biochim Biophys Acta 2001;1514:291–302.

[29] Prasad PD, Wang H, Huang W, Kekuda R, Rajan DP, Leibach FH, et al. Human LAT1, a subunit of system L amino acid transporter: molecular cloning and transport function. Biochem Biophys Res Commun 1999; 255:283–8.

[30] Pineda M, Fernandez E, Torrents D, Estevez R, Lopez C, Camps M, et al. Identification of a membrane protein, LAT-2, that co-expresses with 4F2 heavy chain, an L-type amino acid transport activity with broad specificity for small and large zwitterionic amino acids. J Biol Chem 1999;274:19738–44.

[31] Rossier G, Meier C, Bauch C, Summa V, Sordat B, Verrey F, et al. LAT2, a new basolateral 4F2hc/CD98-associated amino acid transporter of kidney and intestine. J Biol Chem 1999;274:34948–54.

[32] Tsukada H, Sato K, Fukumoto D, Kakiuchi T. Evaluation of D-isomers of *O*-^{18}F-fluoromethyl, *O*-^{18}F-fluoroethyl and *O*-^{18}F-fluoropropyl tyrosine as tumour imaging agents in mice. Eur J Nucl Med Mol Imaging 2006;33:1017–24.

[33] Tsukada H, Sato K, Fukumoto D, Nishiyama S, Harada N, Kakiuchi T. Evaluation of D-isomers of *O*-^{11}C-methyl tyrosine and *O*-^{18}F-fluoromethyl tyrosine as tumor-imaging agents in tumor-bearing mice: comparison with L- and D-^{11}C-methionine. J Nucl Med 2006; 47:679–88.

[34] Gitlitz PH, Sunderman Jr FW, Hohnadel DC. Ion-exchange chromatography of amino acids in sweat collected from healthy subjects during sauna bathing. Clin Chem 1974;20:1305–12.

[35] Oberdorfer F, Hull WE, Traving BC, Maier-Borst W. Synthesis and purification of 2-deoxy-2-[^{18}F]fluoro-D-glucose and 2-deoxy-2-[^{18}F]fluoro-D-mannose: characterization of products by ^{1}H- and ^{19}F-NMR spectroscopy. Int J Rad Appl Instrum [A] 1986;37: 695–701.

[36] Takeda A, Tamano H, Oku N. Alteration of zinc concentrations in the brain implanted with C6 glioma. Brain Res 2003;965:170–3.

[37] Fernstrom JD, Larin F, Wurtman RJ. Daily variations in the concentrations of individual amino acids in rat plasma. Life Sci Pt 1971;10:813–9.

[38] Williams WM, Huang KC. Structural specificity in the renal tubular transport of tyrosine. J Pharmacol Exp Therapeut 1981;219:69–74.

[39] Kubota T. Metastatic models of human cancer xenografted in the nude mouse: the importance of orthotopic transplantation. J Cell Biochem 1994;56:4–8.

Journal of the American College of Cardiology
© 2009 by the American College of Cardiology Foundation
Published by Elsevier Inc.

Vol. 53, No. 8, 2009
ISSN 0735-1097/09/$36.00
doi:10.1016/j.jacc.2008.11.014

PRE-CLINICAL RESEARCH

Prolonged Targeting of Ischemic/Reperfused Myocardium by Liposomal Adenosine Augments Cardioprotection in Rats

Hiroyuki Takahama, MD,*†‡ Tetsuo Minamino, MD, PHD,§ Hiroshi Asanuma, MD, PHD,† Masashi Fujita, MD, PHD,§ Tomohiro Asai, PHD,¶ Masakatsu Wakeno, MD, PHD,*†‡ Hideyuki Sasaki, MD,*†‡ Hiroshi Kikuchi, PHD,# Kouichi Hashimoto,** Naoto Oku, PHD,¶ Masanori Asakura, MD, PHD,† Jiyoong Kim, MD,† Seiji Takashima, MD, PHD,§ Kazuo Komamura, MD, PHD,‖ Masaru Sugimachi, MD, PHD,‖ Naoki Mochizuki, MD, PHD,*‡ Masafumi Kitakaze, MD, PHD, FACC†

Osaka, Shizuoka, and Tokyo, Japan

Objectives The purpose of this study was to investigate whether liposomal adenosine has stronger cardioprotective effects and fewer side effects than free adenosine.

Background Liposomes are nanoparticles that can deliver various agents to target tissues and delay degradation of these agents. Liposomes coated with polyethylene glycol (PEG) prolong the residence time of drugs in the blood. Although adenosine reduces the myocardial infarct (MI) size in clinical trials, it also causes hypotension and bradycardia.

Methods We prepared PEGylated liposomal adenosine (mean diameter 134 ± 21 nm) by the hydration method. In rats, we evaluated the myocardial accumulation of liposomes and MI size at 3 h after 30 min of ischemia followed by reperfusion.

Results The electron microscopy and ex vivo bioluminescence imaging showed the specific accumulation of liposomes in ischemic/reperfused myocardium. Investigation of radioisotope-labeled adenosine encapsulated in PEGylated liposomes revealed a prolonged blood residence time. An intravenous infusion of PEGylated liposomal adenosine (450 μg/kg/min) had a weaker effect on blood pressure and heart rate than the corresponding dose of free adenosine. An intravenous infusion of PEGylated liposomal adenosine (450 μg/kg/min) for 10 min from 5 min before the onset of reperfusion significantly reduced MI size (29.5 ± 6.5%) compared with an infusion of saline (53.2 ± 3.5%, $p < 0.05$). The antagonist of adenosine A_1, A_{2a}, A_{2b}, or A_3 subtype receptor blocked cardioprotection observed in the PEGylated liposomal adenosine-treated group.

Conclusions An infusion as PEGylated liposomes augmented the cardioprotective effects of adenosine against ischemia/reperfusion injury and reduced its unfavorable hemodynamic effects. Liposomes are promising for developing new treatments for acute MI. (J Am Coll Cardiol 2009;53:709–17) © 2009 by the American College of Cardiology Foundation

Liposomes are now widely used for drug delivery in cancer treatment to target specific organs actively or passively and to prevent the degradation of chemotherapy agents (1). However, the application of liposomes for cardiovascular diseases is still limited. In ischemic/reperfused myocardium,

See page 718

cellular permeability is enhanced and vascular endothelial integrity is disrupted (2,3), suggesting that nanoparticles

*From the Department of Molecular Imaging in Cardiovascular Medicine, Osaka University Graduate School of Medicine, Osaka, Japan; †Department of Cardiovascular Medicine, National Cardiovascular Center, Osaka, Japan; ‡Department of Structural Analysis, Research Institute, National Cardiovascular Center, Osaka, Japan; §Department of Cardiovascular Medicine, Osaka University Graduate School of Medicine, Osaka, Japan; ‖Department of Cardiovascular Dynamics, Research Institute, National Cardiovascular Center, Osaka, Japan; ¶Department of Medical Biochemistry, School of Pharmaceutical Sciences, University of Shizuoka, Shizuoka, Japan; #Daiichi Pharmaceutical Co., Tokyo, Japan; and the **Daiichi-Sankyo Pharmaceutical Co., Tokyo, Japan. Supported by a grant for Scientific Research and a grant for the Advancement of Medical Equipment from the Japanese Ministry of Health, Labor, and Welfare, as well as a grant from the Japan Cardiovascular Research Foundation.

Manuscript received September 4, 2008; revised manuscript received October 21, 2008, accepted November 3, 2008.

JACC Vol. 53, No. 8, 2009
February 24, 2009:709–17

Abbreviations and Acronyms

8-SPT = 8-(*p*-sulfophenyl) theophylline
EM = electron microscopy
MI = myocardial infarction
PEG = polyethylene glycol
RI = radioisotope
TTC = triphenyltetrazolium chloride

such as liposomes may be a promising drug delivery system for targeting damaged myocardium with cardioprotective agents. Additionally, coating liposomes with polyethylene glycol (PEG) prolongs their residence time in the circulation (1). Because enhanced microvascular permeability persists for at least 48 h after the occurrence of myocardial infarction (MI) (2), drugs delivered in PEGylated liposomes should be able to display their maximum beneficial effects on myocardial damage after MI.

Adenosine has multiple physiological functions that are mediated via the adenosine A_1, A_{2a}, A_{2b}, and A_3 receptors (4,5). Although large-scale clinical trials suggested the potential value of adenosine therapy for patients with acute MI (6,7), this agent has an extremely short half-life (1 to 2 s) and causes hypotension and bradycardia because of vasodilatory and negative chronotropic effects (4). Because a high dose of adenosine is required to exert cardioprotective effects, it is difficult to use clinically because of the associated hemodynamic consequences. Therefore, we hypothesized that adenosine encapsulated in PEGylated liposomes would cause less hemodynamic disturbance and might also specifically accumulate in ischemic/reperfused myocardium, leading to augmented cardioprotective effects. To test this hypothesis, we created PEGylated liposomal adenosine by the hydration method and investigated: 1) whether liposomal adenosine accumulated in ischemic/reperfused myocardium and prolonged blood residence time; 2) whether liposomal adenosine caused less severe hypotension and bradycardia than free adenosine; and 3) which adenosine receptor subtype was involved in mediating the cardioprotective effects of liposomal adenosine against ischemia/reperfusion injury.

Methods

Materials. The materials for preparing PEGylated liposomes, including hydrogenated soy phosphatidyl choline (HSPC), 1,2-distearoyl-sn-glycero-3-phosphoethanolamine-n-[methoxy (polyethylene glycol)-2000] (DSPE-PEG2000), and cholesterol were obtained from Nissei Oil Co., Ltd. (Tokyo, Japan) and Wako Pure Chemical Co., Ltd. (Osaka, Japan). [^{3}H]-adenosine was purchased from Daiichi Pure Chemicals Co., Ltd. (Tokyo, Japan). Other materials were obtained from Sigma (St. Louis, Missouri), including 8-(*p*-sulfophenyl)theophylline (8-SPT; a nonselective adenosine receptor antagonist), 1,3-diethyl-8-phenylxanthine (DPCPX; a selective adenosine A_1 receptor antagonist), 5-amino-7-(phenylethyl)-2-(2-furyl)-pyrazolo[4,3-e]-1,2,4-triazolo[1,5-c] pyrimidine (SCH58261; a selective adenosine A_{2a} receptor antagonist), 8-[4-[((4-cyanophenyl)carbamoylmethyl) oxy]phenyl]-1, 3-di(n-propyl)xanthine (MRS1754; a selective adenosine A_{2b} receptor antagonist), and 5-propyl-2-ethyl-4-propyl-3-(ethylsulfanylcarbonyl)-6-phenylpyridine-5-carboxylate (MRS1523, a selective adenosine A_3 receptor antagonist).

Animals. Male Wistar rats (9 weeks old and weighing 250 to 310 g, Japan Animals, Osaka, Japan) were used. The animal experiments were approved by the National Cardiovascular Center Research Committee and were performed according to institutional guidelines.

Preparation of PEGylated liposomes. The PEGylated liposomes were prepared by the hydration method. Briefly, adenosine was added to the lipid solution. After mixture of lipid and adenosine, DSPE-PEG2000 was added and incubated. The final composition of PEGylated liposomes was HSPC:cholesterol:DSPE-PEG2000 = 6.0:4.0:0.3 (molar ratio). After ultracentrifugation several times, the pellet of liposomal adenosine was resuspended in sodium lactate at each required concentration for use in the experimental protocols. Some samples of final liposomal adenosine were disrupted by dilution with 50% methanol (1.5 ml per 30-μl of liposomes). After 10 min of ultracentrifugation, the concentration of adenosine in the supernatant was measured by high-performance liquid chromatography.

To prepare fluorescent-labeled liposomes, 0.5 mol% tetramethylrhodamine isothiocyanate (rhodamine) was added to the lipid mixture. To prepare radioisotope (RI)-labeled adenosine encapsulated in liposomes, [^{3}H]-radiolabeled adenosine (Daiichi Pure Chemicals, Tokyo, Japan) was diluted with free adenosine and was encapsulated in liposomes as described above.

Characterization of PEGylated liposomal adenosine. The characterization of the liposomes was performed by the dynamic scatter analysis (Zetasizer Nano ZS, Malvern, Worcestershire, United Kingdom). The analyses were performed 10 times per sample, and results represented analyses of 4 independent experiments.

Experimental protocols. PROTOCOL 1: EFFECTS OF PEGYLATED LIPOSOMAL ADENOSINE ON HEMODYNAMICS IN RATS. Rats were anesthetized with intraperitoneal sodium pentobarbital (50 mg/kg). Catheters were advanced into a femoral artery and vein for the measurement of systemic blood pressure and infusion of drugs, respectively. Both blood pressure and heart rate were monitored continuously during the study using a Power Lab (AD Instruments, Castle Hill, Australia). After hemodynamics became stable, we intravenously administered empty PEGylated liposomes (n = 8), free adenosine (n = 8), or PEGylated liposomal adenosine (n = 8) for 10 min. Either PEGylated liposomal or free adenosine was infused at an initial dose of 225 μg/kg/min (0.1 ml/min) for 10 min. After a 5-min interval, either PEGylated liposomal adenosine or free adenosine was infused at 450 μg/kg/min (0.1 ml/min) for 10 min. In the same manner, PEGylated liposomal adenosine or free adenosine was then infused at 900 μg/kg/min (0.1 ml/min).

PROTOCOL 2: EFFECTS OF PEGYLATED LIPOSOMAL ADENOSINE ON INFARCT SIZE IN RATS. The MI was induced by transient ligation of the left coronary artery as described previously (8). In the first series of experiments, to examine the dose-dependent effects of liposomal adenosine on MI size, PEGylated liposomal adenosine was infused intravenously at 50, 150, or 450 μg/kg/min for a 10-min period starting from 5 min before the onset of reperfusion. In the second series of experiments, to determine the adenosine receptor subtype involved in cardioprotective effects by the liposomal adenosine, the antagonist of adenosine subtype receptor was intravenously injected as a bolus followed by the infusion of liposomal adenosine for 10 min. The MI size was evaluated at 3 h after the start of reperfusion. The doses of adenosine receptor subtype antagonists were determined according to the previous reports (9–11).

Measurement of infarct size. At 3 h after the onset of reperfusion, the area at risk and the infarcted area were determined by Evans blue and triphenyltetrazolium chloride (TTC) staining, respectively, as previously described (8). Infarct size was calculated as [infarcted area/area at risk] × 100(%) in a blind manner. The area at risk was composed of border (TTC staining) and infarcted (TTC nonstaining) areas.

Electron microscopy (EM). Myocardial samples for EM were obtained from the central and peripheral areas in ischemic/reperfused myocardium, which roughly corresponded to the infarcted and border areas, respectively, after the left coronary artery was occluded for 30 min of ischemia followed by 3 h of reperfusion. Samples were prepared as previously reported (12). Liposomes, whose major membrane component is unsaturated phospholipids, were visualized as homogenous dark dots with a diameter of 100 to 150 nm (13).

Accumulation of fluorescent-labeled PEGylated liposomes in ischemic/reperfused myocardium. Unlabeled or fluorescent-labeled PEGylated liposomes were infused intravenously at a dose of 0.1 ml/min as liposomal adenosine was infused in protocol 2. At 3 h after reperfusion, hearts were quickly removed and cut into 4 sections parallel to the axis from base to apex. Then ex vivo bioluminescence imaging was performed with an Olympus OV 100 imaging system (Olympus, Tokyo, Japan) and signals were quantified using WASABI quantitative software (Hamamatsu Photonics K.K., Shizuoka, Japan). Fluorescent intensity in the region of interest was measured as previously reported (14). Control intensity indicated the fluorescent intensity in the nonischemic area of the individual rat.

Time-course changes of free and PEGylated liposomal RI-labeled adenosine in plasma and myocardium. Free or PEGylated liposomal [^{3}H]-adenosine (83 kBq per rat) was infused intravenously at a dose of 0.1 ml/min as liposomal adenosine was infused in protocol 2. At the time indicated, rat hearts were harvested for counting of radioactivity (LSC-3100, Aloka Co., Tokyo, Japan). Results are expressed as a percentage of the injected dose per 1 ml of blood or 1 g of wet tissue weight.

Statistical analysis. The parameters of the liposomes were expressed as the average ± SD, whereas other data were expressed as the average ± SEM. Comparison of time-course changes in hemodynamic parameters between groups was performed by 2-way repeated-measures analysis of variance (ANOVA) followed by a post-hoc Bonferroni test. For comparison of RI activity between groups, statistical analysis was done with the Mann-Whitney *U* test. To address the differences in infarct size among groups, we performed a nonparametric (Kruskal-Wallis) test followed by evaluation with the Mann-Whitney *U* test. Resulting p values were corrected according to the Bonferroni method. To compare parameters of liposomes, an unpaired *t* test was performed. In all analyses, $p < 0.05$ was considered to indicate statistical significance.

Results

Characterization of liposomes by dynamic light scatter analysis. The dynamic light scatter analysis showed no significant difference in mean diameter, polydispersity index, or zeta-potential distribution between empty and adenosine-loaded PEGylated liposomes (Table 1).

Liposomes in ischemic/reperfused myocardium. The EM revealed the intact vascular endothelial cells and cardiomyocytes in the nonischemic myocardium (Figs. 1A and 1B). There were no homogenous dark dots indicating liposomes in the nonischemic myocardium of rats that received either saline (Fig. 1A) or liposomes (Fig. 1B). In the border area, many homogenous dark dots indicating liposomes were accumulated in rats that received liposomes, but not saline (Figs. 1C and 1D). In this area, significant structural damage was not observed in endothelium, but slight swelling of mitochondria was often observed. In the infarcted area, numerous liposomes were detected in rats that received liposomes, but not saline (Figs. 1E and 1F). In this area, the disrupted endothelial integrity and marked swelling of mitochondria were often observed.

Table 1 Characterization of Liposomes by Dynamic Light Scatter Analysis

	Mean Diameter (nm)	Polydispersity Index	Zeta Potential (mV)
PEGylated liposomes (empty liposomes)	126 ± 12	0.035 ± 0.003	−1.7 ± 0.4
PEGylated liposomal adenosine	134 ± 21	0.094 ± 0.002	−2.3 ± 1.1

Results represented analysis of 4 independent experiments. Values are expressed as mean ± SD.
PEG = polyethylene glycol.

JACC Vol. 53, No. 8, 2009
February 24, 2009:709–17

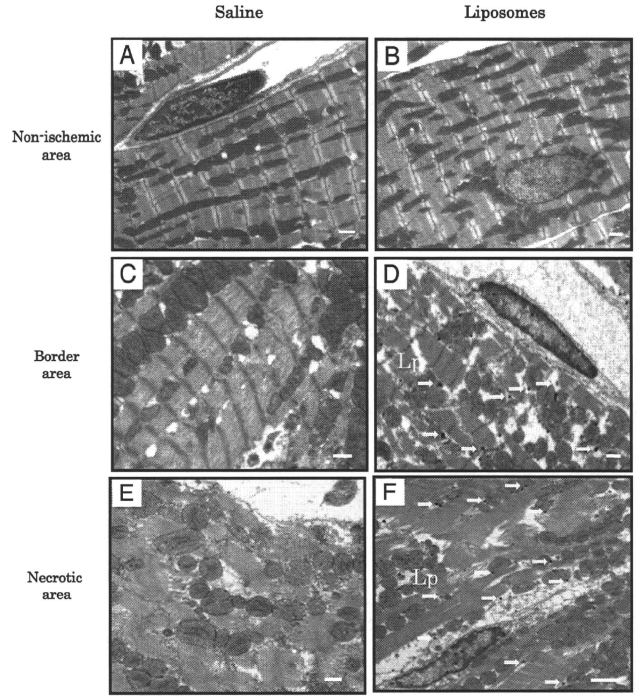

Figure 1 Liposomes in Ischemic/Reperfused Myocardium

(A, B) Representative electron micrographs of the nonischemic area in rats that received saline **(A)** or liposomes (Lp) **(B)**. **(C, D)** Representative electron micrographs of border area at 3 h after myocardial infarction (MI). Many **dark dots** accumulated in this area in the rat that received liposomes but not saline. **(E, F)** Representative electron micrographs of infarcted areas at 3 h after MI. Numerous **dark dots** accumulated in this area in the rat that received liposomes but not saline. Scale bars represent 1 μm.

Fluorescent-labeled PEGylated liposomes in ischemic/reperfused myocardium. Quantitative analysis by bioluminescence ex vivo bioluminescene imaging revealed that the target to control fluorescent intensity ratio was higher in the border (noninfarcted area at risk) as well as infarcted areas compared with a nonischemic one, suggesting that fluorescent-labeled liposomes were accumulated in the border as well as infarcted areas. Since there was no high-intensity area when unlabeled liposomes were infused, it was suggested that this was not a nonspecific phenomenon to MI by the ex vivo bioluminescence imaging system (Fig. 2). The Evans blue staining was unrelated to the fluorescence intensity (data not shown).

Plasma radioactivity of RI-labeled adenosine was markedly higher in the PEGylated liposomal adenosine group at 10 min and 3 h after the intravenous infusion than in the free adenosine group (Fig. 3A). Encapsulation within PEGylated liposomes also augmented the accumulation of adenosine in ischemic/reperfused myocardium compared with that of free adenosine (Fig. 3B).

Hemodynamic effects of PEGylated liposomal adenosine. Baseline hemodynamic parameters did not differ among the groups. An intravenous infusion of free adenosine at doses of 225, 450, and 900 μg/kg/min decreased the mean blood pressure by 14.8%, 25.4%, and 33.7%, respectively, compared with the effect of empty PEGylated lipo-

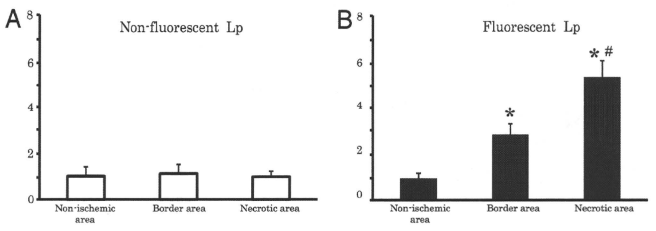

Figure 2 **Detection of Fluorescence-Labeled PEGylated Liposomes in Ischemic/Reperfused Myocardium**

Quantitative analysis of target-to-control fluorescent intensity ratio for each area in rats (n = 3 each group) that received nonfluorescent **(A)** or fluorescent **(B)** liposomes. The values of bioluminescence signals in the border and infarcted areas were expressed as the fold to that of the each nonischemic area. Values are expressed as the mean ± SEM (error bars). *p < 0.05 versus nonischemic areas. #p < 0.05 versus border areas.

somes. In contrast, the intravenous infusion of PEGylated liposomal adenosine at a dose of either 225 or 450 μg/kg/min did not significantly alter mean blood pressure (Fig. 4). Changes of the heart rate after infusion of PEGylated liposomal adenosine or free adenosine were similar to those observed for mean blood pressure (Fig. 4).

Effects of PEGylated liposomal adenosine on MI size. Baseline hemodynamic parameters were similar among all of the groups (Table 2). Intravenous infusion of free adenosine for 10 min reduced both the blood pressure and the heart rate, although these parameters returned to baseline within 5 min of ceasing infusion (Table 2). In contrast, hemodynamic parameters of the other groups were not altered (Table 2). The area at risk in the control group (61 ± 3%) did not differ compared with those of other groups that received liposomal adenosine. Intravenous infusion of PEGylated liposomal adenosine caused a dose-dependent decrease of MI size compared with that in the control group, whereas intravenous infusion of empty PEGylated liposomes or free adenosine did not (Fig. 5B).

The bolus injection of adenosine receptor antagonist did not alter the hemodynamic parameters (Table 3). The area at risk in the liposomal adenosine group (58 ± 3%) did not differ compared with those of other groups that received adenosine receptor antagonist. Infusion of 8-SPT, a nonspecific adenosine receptor antagonist, blunted the cardioprotective effect of liposomal adenosine (Fig. 6B). Furthermore, the infusion of the adenosine A_1, A_{2a}, A_{2b}, or A_3 receptor antagonist also blunted cardioprotective effects of liposomal adenosine (Fig. 6B). Infusion of 8-SPT alone did not significantly affect myocardial infarct size compared with the control (52 ± 5%, n = 4).

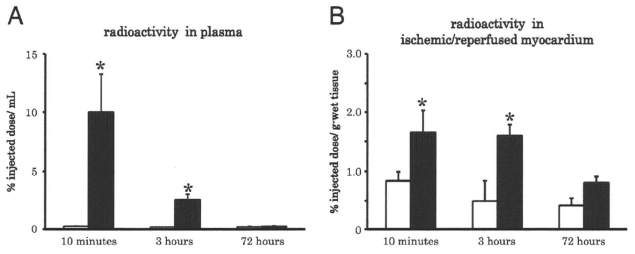

Figure 3 **Radioisotope-Labeled Adenosine in Plasma and Ischemic/Reperfused Myocardium**

(A) Changes in plasma radioactivity after infusion of radioisotope-labeled adenosine. **Solid and open bars** indicate the PEGylated liposomal adenosine and free adenosine groups, respectively (n = 4 each). In the PEGylated liposomal adenosine group, plasma radioactivity was markedly higher than in the free adenosine group. **(B)** Changes in radioactivity in ischemic/reperfused myocardium. **Solid and open bars** indicate the PEGylated liposomal adenosine and free adenosine groups, respectively (n = 4 each). In the PEGylated liposomal adenosine group, myocardial radioactivity was markedly higher than in the free adenosine group. Values are expressed as the mean ± SEM (error bars). *p < 0.05 versus the free adenosine group at the corresponding time.

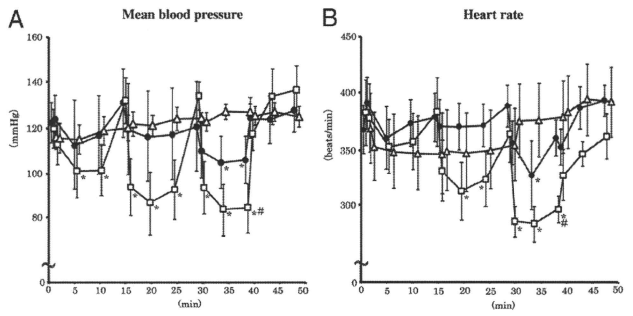

Figure 4 **Hemodynamic Effects of PEGylated Liposomal Adenosine**

Changes in the mean blood pressure **(A)** and heart rate **(B)** after intravenous infusion of various doses of empty PEGylated liposomes **(triangles)**, PEGylated liposomal adenosine **(circles)**, or free adenosine **(squares)** (n = 8 each). Values are expressed as the mean ± SEM. *p < 0.05 versus baseline at the corresponding group. #p < 0.05 versus PEGylated liposomes.

Discussion

In the present study, EM, bioluminescence ex vivo imaging, and fluorescent analysis revealed the accumulation of liposomes in the border (noninfarcted areas at risk) as well as infarcted ones, but not nonischemic myocardium, at 3 h after MI. These findings suggested that liposomes could specifically accumulate in ischemic/reperfused myocardium. Interestingly, EM revealed the existence of liposomes at sites where endothelial integrity was still morphologically maintained. Endothelial dysfunction such as enhanced permeability is induced by ischemic insult without morphological endothelial disruption (3,15). Enhanced permeability might lead to the accumulation of liposomes in the border as well as infarcted area, which will contribute to salvage the ischemic/reperfused myocardium. However, further investigation will be needed to determine the precise mechanism by which liposomes accumulate in ischemic/reperfused myocardium.

Analysis using RI-labeled adenosine encapsulated in liposomes revealed that plasma radioactivity was markedly higher in the PEGylated liposomal adenosine group compared with the free adenosine group. This indicates that encapsulation of adenosine by PEGylated liposomes considerably prolonged its residence time in the circulation and delayed its degradation. Consistent with the histological data, RI-labeled adenosine also showed preferential accumulation in ischemic/reperfused myocardium.

Table 2 **Effects of Liposomal Adenosine on Hemodynamic Parameters**

		Ischemia				Reperfusion	
	Baseline	**0 min**	**15 min**	**25 min**	**30 min**	**5 min**	**10 min**
Mean blood pressure (mm Hg)							
Saline	122 ± 5	102 ± 10	108 ± 7	107 ± 9	108 ± 7	105 ± 9	104 ± 9
Vehicle	127 ± 4	109 ± 8	108 ± 7	111 ± 9	111 ± 5	105 ± 5	103 ± 5
Free-Ado	124 ± 8	115 ± 8	111 ± 5	109 ± 4	66 ± 4*	62 ± 4*	112 ± 6
Lp-Ado 50 μg/kg/min	121 ± 5	106 ± 6	105 ± 6	110 ± 10	102 ± 6	101 ± 6	104 ± 4
Lp-Ado 150 μg/kg/min	122 ± 3	107 ± 6	107 ± 6	109 ± 11	105 ± 6	100 ± 6	103 ± 4
Lp-Ado 450 μg/kg/min	124 ± 3	104 ± 6	105 ± 6	107 ± 5	102 ± 6	99 ± 6	104 ± 4
Heart rate (beats/min)							
Saline	363 ± 22	366 ± 19	369 ± 14	413 ± 22	372 ± 12	372 ± 16	371 ± 14
Vehicle	363 ± 32	363 ± 6	383 ± 6	396 ± 25	367 ± 6	374 ± 7	372 ± 7
Free-Ado	360 ± 18	361 ± 17	384 ± 13	379 ± 18	305 ± 11*	293 ± 13*	356 ± 14
Lp-Ado 50 μg/kg/min	378 ± 19	386 ± 21	366 ± 12	376 ± 12	367 ± 19	369 ± 9	377 ± 17
Lp-Ado 150 μg/kg/min	388 ± 27	376 ± 20	371 ± 14	377 ± 13	378 ± 16	373 ± 16	369 ± 17
Lp-Ado 450 μg/kg/min	368 ± 17	376 ± 21	361 ± 13	386 ± 15	368 ± 15	363 ± 6	367 ± 7

Values are expressed as mean ± SEM. *p < 0.05 versus baseline.
Free-Ado = free adenosine; Lp-Ado = PEGylated liposomal adenosine; PEG = polyethylene glycol; vehicle = PEGylated liposomes.

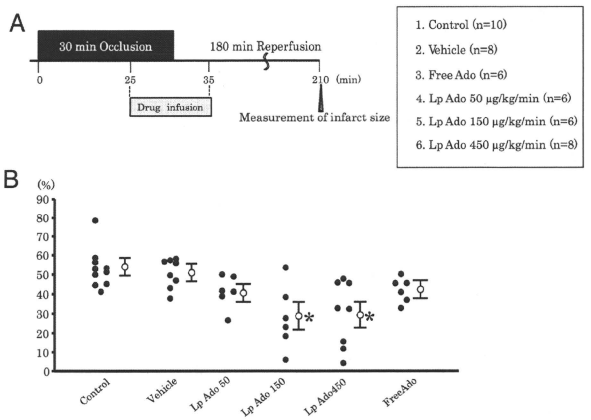

Figure 5 Dose-Dependent Effects of PEGylated Liposomal Adenosine on Myocardial Infarct Size

(A) Protocol showing the timing of infusion of PEGylated liposomal adenosine and of infarct size measurement. **(B)** Myocardial infarct size. Values are expressed as mean ± SEM (error bars). *$p < 0.05$ versus the control group. Free-Ado = free adenosine; Lp-Ado = PEGylated liposomal adenosine; Vehicle = PEGylated liposomes.

Furthermore, this study showed that PEGylated liposomal adenosine had a weaker effect on the blood pressure and heart rate than free adenosine. Thus, encapsulating adenosine in PEGylated liposomes attenuated its vasodilatory and negative chronotropic effects, presumably by reducing the amount of circulating free adenosine. However, the changes of hemodynamic parameters in this in vivo model suggested that significant release of adenosine from PEGylated liposomes would still occur if a large dose of liposomal adenosine (e.g., 900 μg/kg/min) were administered. Thus, further investigation of the in vivo pharmacodynamics of PEGylated liposomal adenosine is needed.

An intravenous infusion of PEGylated liposomal adenosine at the maximum dose that did not disturb hemodynamic parameters for 10 min before reperfusion reduced MI size in a dose-dependent manner, and this improvement was blocked by 8-SPT, a nonselective adenosine receptor antagonist. These findings suggest that adenosine released from liposomes acts via an adenosine receptor-dependent pathway. One possible mechanism by which PEGylated lipo-

Table 3 Effects of Adenosine Receptor Antagonist on Hemodynamic Parameters

		Ischemia				Reperfusion	
	Baseline	0 min	15 min	25 min	30 min	5 min	10 min
Mean blood pressure (mm Hg)							
Lp-Ado + 8SPT	120 ± 6	113 ± 4	112 ± 6	112 ± 5	107 ± 6	102 ± 8	109 ± 7
Lp-Ado + DPCPX	130 ± 6	105 ± 4	121 ± 4	100 ± 10	122 ± 6	120 ± 6	111 ± 4
Lp-Ado + SCH58261	132 ± 2	98 ± 12	99 ± 8	110 ± 8	118 ± 10	113 ± 10	109 ± 6
Lp-Ado + MRS1754	130 ± 3	95 ± 12	106 ± 8	105 ± 10	100 ± 10	96 ± 10	99 ± 7
Lp-Ado + MRS1523	130 ± 2	109 ± 8	104 ± 8	105 ± 9	100 ± 9	101 ± 10	104 ± 6
Heart rate (beats/min)							
Lp-Ado + 8SPT	404 ± 17	385 ± 10	374 ± 8	396 ± 8	389 ± 9	383 ± 8	385 ± 9
Lp-Ado + DPCPX	396 ± 24	380 ± 11	399 ± 9	398 ± 12	385 ± 9	382 ± 9	380 ± 7
Lp-Ado + SCH58261	393 ± 14	399 ± 15	381 ± 9	395 ± 15	376 ± 9	373 ± 9	385 ± 7
Lp-Ado + MRS1754	398 ± 14	392 ± 11	401 ± 9	379 ± 15	378 ± 9	374 ± 9	377 ± 7
Lp-Ado + MRS1523	396 ± 9	390 ± 11	390 ± 11	392 ± 10	373 ± 9	391 ± 7	388 ± 11

Values were expressed as mean ± SEM. *$p < 0.05$ versus baseline.
Lp-Ado = PEGylated liposomal adenosine; PEG = polyethylene glycol; Vehicle = PEGylated liposomes.

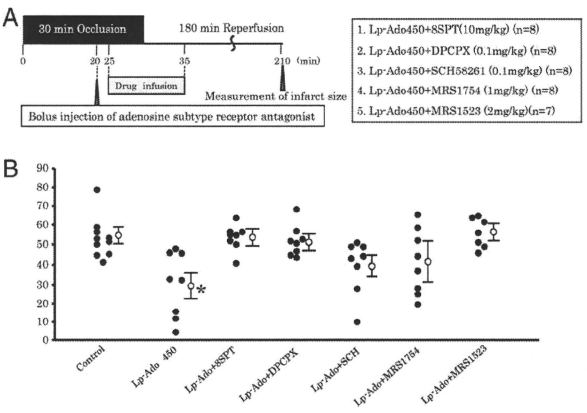

Figure 6 **Effects of Adenosine Receptor Antagonists on Myocardial Infarct Size**

(A) Protocol showing the timing of infusion of PEGylated liposomal adenosine and bolus injection adenosine receptor antagonists. **(B)** Myocardial infarct size. Values are expressed as the mean ± SEM (error bars). *$p < 0.05$ versus the control group. The abbreviations for adenosine antagonists were described in the text. Abbreviations as in Figure 5.

somes could augment cardioprotective effects of liposomal adenosine with minimum effects on hemodynamic parameters is the enhanced accumulation of PEGylated liposomal adenosine in ischemic/reperfused myocardium, which could augment various beneficial actions such as preventing calcium overload in the myocardium (5). The prolonged persistence of PEGylated liposomal adenosine would also increase its beneficial effect on ischemic/reperfused myocardium. Although continuous high-dose, long-term infusion of free adenosine was reported to reduce infarct size in rats (16), the present study did not confirm such a cardioprotective effect, probably because the total dose of free adenosine that we used was not high enough.

We found that myocardial infarct size in the group that received PEGylated liposomal adenosine with the antagonist of adenosine A_1, A_{2a}, A_{2b}, or A_3 subtype receptor was no different from the control group, indicating that every adenosine subtype receptor could possibly play a role in mediating cardioprotection by liposomal adenosine and that it was difficult to identify one particular subtype in the present study. Numerous studies reported that A_1, A_{2a}, A_{2b}, and A_3 receptors have been involved in cardioprotection against ischemia/reperfusion injury, and it remains controversial which adenosine subtype receptor is most responsible for cardioprotection (17–20). Furthermore, because the adenosine receptor antagonists used in the present study had some nonspecific effects, future investigation will be needed to examine the precise role of each adenosine receptor subtype using genetically engineered mice.

Because liposomal adenosine infused during reperfusion could reduce MI size, this agent could be a candidate for the adjunctive therapy of patients with acute MI. Importantly, adenosine is currently used for the diagnosis of ischemic heart disease and PEGylated liposomes are used to deliver anticancer agents (21). Thus, it should not be difficult to introduce PEGylated liposomal adenosine into clinical practice. Finally, PEGylated liposomes may provide a useful drug delivery system for targeting ischemic/reperfused myocardium with other agents.

Acknowledgments

The authors thank Akiko Ogai and Yoko Nakano for their excellent technical assistance; Motohide Takahama, Hiroyuki Hao, and Hatsue Ishibashi-Ueda for advice about the electron microscopy figure; and Syunichi Kuroda and Takashi Matsuzaki for assistance with bioluminescence imaging.

Reprint requests and correspondence: Dr. Tetsuo Minamino, Department of Cardiovascular Medicine, Osaka University Graduate School of Medicine, 2-2 Yamadaoka, Suita, Osaka 565-0871, Japan. E-mail: minamino@medone.med.osaka-u.ac.jp.

REFERENCES

1. Papahadjopoulos D, Allen TM, Gabizon A, et al. Sterically stabilized liposomes: improvements in pharmacokinetics and antitumor therapeutic efficacy. Proc Natl Acad Sci U S A 1991;24:11460–4.

2. Horwitz LD, Kaufman D, Keller MW, Kong Y. Time course of coronary endothelial healing after injury due to ischemia and reperfusion. Circulation 1994;90:2439–47.
3. Dauber IM, Van Benthuysen KM, McMurtry IF, et al. Functional coronary microvascular injury evident as increased permeability due to brief ischemia and reperfusion. Circ Res 1990;66:986–98.
4. Forman MB, Stone GW, Jackson EK. Role of adenosine as adjunctive therapy in acute myocardial infarction. Cardiovasc Drug Rev 2006;24:116–47.
5. Mubagwa K, Flameng W. Adenosine, adenosine receptors and myocardial protection: an updated overview. Cardiovasc Res 2001;52:25–39.
6. Mahaffey KW, Pume JA, Barbagelata NA, et al. Adenosine as an adjunct to thrombolytic therapy for acute myocardial infarction: results of a multicenter, randomized, placebo-controlled trial: the Acute Myocardial Infarction STudy of ADenosine (AMISTAD) trial. J Am Coll Cardiol 1999;34:1711–20.
7. Ross AM, Gibbons RJ, Stone GW, Kloner RA, Alexander RW, for the AMISTAD-II ÂInvestigators. A randomized, double-blinded, placebo-controlled multicenter trial of adenosine as an adjunct to reperfusion in the treatment of acute myocardial infarction (AMISTAD-II). J Am Coll Cardiol 2005;45:1775–80.
8. Bullard AJ, Govewalla P, Yellon DM. Erythropoietin protects the myocardium against reperfusion injury in vitro and in vivo. Basic Res Cardiol 2005;100:397–403.
9. Hannon JP, Tigani B, Wolber C, et al. Evidence for an atypical receptor mediating the augmented bronchoconstrictor response to adenosine induced by allergen challenge in activity sensitized Brown Norway rats. Br J Pharmacol 2002;135:685–96.
10. Kin H, Zatta AJ, Lofye MT, et al. Postconditioning reduces infarct size via adenosine receptor activation by endogenous adenosine. Cardiovasc Res 2005;67:124–33.
11. Hinschen AK, RoseMeyer RB, Headrick JP. Adenosine receptor subtypes mediating coronary vasodilation in rat hearts. J Cardiovasc Pharmacol 2003;41:73–80.
12. Kaeffeer N, Richard V, Francois A, Lallemand F, Henry JP, Thuillez C. Preconditioning prevents chronic reperfusion-induced coronary endothelial dysfunction in rats. Am J Physiol 1996;271:H842–9.
13. M Shimizu, Miwa K, Hashimoto Y, Goto A. Encapsulating of chicken egg yolk immunoglobulin G (IgY) by liposomes. Biosci Biotechnol Biochem 1993;57:1445–9.
14. Kasuya T, Jung J, Kadoya H, et al. In vivo delivery of bionanocapsules displaying phaseolus vulgaris agglutinin-L(4) isolectin to malignant tumors overexpressing N-acetylglucosaminlyltransferase V. Hum Gene Ther 2008;19:887–95.
15. Kim YD, Fomsgaard JS, Heim KF, et al. Brief ischemia-reperfusion induces stunning of endothelium in canine coronary artery. Circulation 1992;85:1473–82.
16. Canyon SJ, Dobson GP. Protection against ventricular arrhythmias and cardiac death using adenosine and lidocaine during regional ischemia in the in vivo rat. Am J Physiol Heart Circ Physiol 2004;287:H1286–95.
17. Yaar R, Jones MR, Chen JF, Ravid K. Animal models for the study of adenosineÂreceptor function. J Cell Physiol 2005;202:9–20.
18. Norton ED, Jackson EK, Turner MB, Virmani R, Forman MB. The effects of intravenous infusions of selective adenosine A_1-receptor and A_2-receptor agonists on myocardial reperfusion injury. Am Heart J 1992;123:332–8.
19. Xu Z, Mueller RA, Park SS, Boysen PG, Cohen MV, Downey JM. Cardioprotection with adenosine A_2 receptor activation at reperfusion. J Cardiovasc Pharmacol 2005;46:794–802.
20. Vinten-Johansen J. Postconditioning: a mechanical maneuver that triggers biological and molecular cardioprotective responses to reperfusion. Heart Fail Rev 2007;12:235–344.
21. Lasic DD. Doxorubicin in sterically stabilized liposomes. Nature 1996;380:561–2.

Key Words: myocardial infarction ▪ liposome ▪ drug delivery system ▪ adenosine.

Artificial Organs

Artificial Organs
33(2):164–168, Wiley Periodicals, Inc.

In Vivo Distribution of Liposome-Encapsulated Hemoglobin Determined by Positron Emission Tomography

*Takeo Urakami, †Akira T. Kawaguchi, ‡Shuji Akai, *Kentaro Hatanaka, *Hiroyuki Koide, *Kosuke Shimizu, *Tomohiro Asai, §Dai Fukumoto, §Norihiro Harada, §Hideo Tsukada, and *Naoto Oku

**Department of Medical Biochemistry and Global COE Program, and ‡Synthetic Organic Chemistry, Graduate School of Pharmaceutical Sciences, University of Shizuoka, Shizuoka; †Tokai University School of Medicine, Isehara, Kanagawa; and §Central Research Laboratory, Hamamatsu Photonics K.K., Hamamatsu, Shizuoka, Japan*

Abstract: Positron emission tomography (PET) is a noninvasive imaging technology that enables the determination of biodistribution of positron emitter-labeled compounds. Lipidic nanoparticles are useful for drug delivery system (DDS), including the artificial oxygen carriers. However, there has been no appropriate method to label preformulated DDS drugs by positron emitters. We have developed a rapid and efficient labeling method for lipid nanoparticles and applied it to determine the movement of liposome-encapsulated hemoglobin (LEH). Distribution of LEH in the rat brain under ischemia was examined by a small animal PET with an enhanced resolution. While the blood flow was almost absent in the ischemic region observed by $[^{15}O]H_2O$ imaging, distribution of ^{18}F-labeled LEH in the region was gradually increased during 60-min dynamic PET scanning. The results suggest that LEH deliver oxygen even into the ischemic brain from the periphery toward the core of ischemia. The real-time observation of flow pattern, deposition, and excretion of LEH in the ischemic rodent brain was possible by the new methods of positron emitter labeling and PET system with a high resolution.
Key Words: Liposome-encapsulated hemoglobin—Positron emission tomography—Pharmacokinetics—Brain ischemia—Drug delivery system.

Liposome encapsulation has been used for drug delivery system (DDS) in a wide range of applications, including chemotherapeutics (1), photosensitizers (2), and nucleic acid derivatives (3). Recently, human hemoglobin was encapsulated in liposome nanocapsule (liposome-encapsulated hemoglobin [LEH] to be an artificial oxygen carrier as a substitute for red blood cells (RBCs) (4,5). In order to clarify the behavior of LEH in vivo, noninvasive, real-time imaging of their movement is desirable. Positron emission tomography (PET) is a noninvasive technique that has been used for clinical applications for diagnosis, as well as for functional evaluation. This technique can also be applied to pharmacokinetic studies to monitor the distribution and quantification of drugs far more quickly and cost-effectively than the conventional techniques requiring sacrifice and dissection of the animals (6,7). Nonetheless, there have been certain limitations in PET studies, including the labeling with positron emitters, its half-life, and difficulty in handling. When the small molecular-weight compound is a target, the compound has to be labeled directly with positron emitters. When it comes to labeling preformulated drugs such as DDS drugs and LEH, the process of the formulation requires specific facilities and multiple steps, prohibiting labeling the composition of DDS drugs or LEH with positron emitters with short half-lives. Therefore, we have developed a solid-phase transition (SophT) method for labeling preformulated liposomal drugs (8). In the current study, LEH was labeled

doi:10.1111/j.1525-1594.2008.00702.x

Received May 2008; revised October 2008.
Address correspondence and reprint requests to Dr. Naoto Oku, Department of Medical Biochemistry, School of Pharmaceutical Sciences, University of Shizuoka, 52-1 Yada, Suruga-ku, Shizuoka 422-8526, Japan. E-mail: oku@u-shizuoka-ken.ac.jp
Presented in part at the 2007 Joint Congress of Japanese Society for Artificial Organs and the International Federation for Artificial Organs held on October 28–31, 2007 in Osaka, Japan.

with a novel [^{18}F]-probe and SophT method ([^{18}F]-labeled LEH), and administered to rats with cerebral ischemia after photochemically induced thrombosis (PIT) of the middle cerebral artery (MCA) (9). The flow pattern and distribution of LEH in rats with brain ischemia were continuously followed by an enhanced PET imaging system developed for small animal studies (Clairvivo, Shimadzu, Kyoto, Japan) (10).

MATERIALS AND METHODS

Liposome-encapsulated hemoglobin (LEH)

LEH (TRM-645) was supplied from Terumo Co. Ltd. (Tokyo, Japan). Relevant characteristics of the LEH have been reported (5). Briefly, it is a liposome capsule having 230 nm in mean diameter, containing human hemoglobin that had been eluted from RBCs outdated for transfusion. The liposome capsule is coated with polyethylene glycol to reduce aggregation and trapping by the reticuloendothelial system.

Synthesis of a positron emitter-labeled probe, SteP2

The synthesis of 1-[^{18}F]fluoro-3,6-dioxatetracosane (SteP2) was reported elsewhere (8). Briefly, [^{18}F]fluoride was produced with a cyclotron (HM-18, Sumitomo Heavy Industries, Tokyo, Japan) at the Hamamatsu Photonics PET Center, and the labeled compound was synthesized from the precursor (Fig. 1). The radiochemical purity was 100%. Specific radioactivity was not determined because its concentration was below the limit of quantification.

Labeling of LEH

Labeling of LEH was performed by SophT method (8). About 100 MBq of [^{18}F]SteP2 in ethanol solution was transferred to a glass test tube, and the solvent was removed completely at 90°C with helium gas flow. LEH solution was added to the vial with the [^{18}F]-radiolabeled compound and incubated at 37°C for 15 min with 5-s mixing by vortex stirrer every 3 min. After the incubation, LEH solution was centrifuged at 100 000 × g for 15 min (Beckman, Fullerton, CA, USA), and the supernatant was transferred to a new tube. Radioactivity in the original tube for labeling, supernatant, and precipitate was measured by curiemeter (IGC-3, Aloka, Tokyo, Japan) to calculate the labeling efficiency. The effect of SophT method on physical properties of LEH was examined by use of Zetasizer Nano ZX (Malvern, UK).

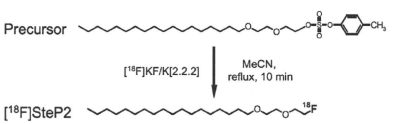

FIG. 1. Synthesis of 1-[^{18}F]fluoro-3,6-dioxatetracosane, [^{18}F]SteP2.

Animal model

In all experiments, rats were maintained and handled subject to the recommendations of the National Institute of Health, the guidelines of the University of Shizuoka, and the guidelines of the Central Research Laboratory, Hamamatsu Photonics. Photochemically-induced thrombosis model was prepared as previously reported with minor modifications (9). Male Sprague-Dawley rats (Japan SLC, Inc., Shizuoka, Japan) were anesthetized and maintained with 2% halothane in a mixture of 70% room air and 30% O_2 throughout the following procedure. After infusion of rose bengal (20 mg/kg), photoillumination (200 000 Lux) was delivered for 20 min to the MCA through the dura by an optic fiber. After confirmation of thrombotic occlusion of the MCA, the incision was closed and transferred to the PET study.

PET imaging of cerebral blood flow (CBF)

Rats were anesthetized with intraperitoneal injection of chloral hydrate at 400 mg/kg, followed by continuous intravenous infusion at 100 mg/kg/h throughout the remaining experiment. To determine the regional CBF, [^{15}O]H_2O (7 MBq in 0.3 mL) was injected via tail vein with the rat fixed on an animal holder. The PET scan was started immediately after the administration of [^{15}O]H_2O and was performed for 2 min using an ultrahigh spatial resolution, small animal PET system, Clairvivo.

PET imaging of [^{18}F]-labeled LEH

Twenty minutes after the administration of [^{15}O]H_2O, LEH labeled with ^{18}F positron emitter was injected into rats through the tail vein. The PET scan was started immediately after injection of the labeled LEH (7 MBq) and was continuously performed for 60 min. The radioactivity in the form of coincidence gamma photons was measured and converted to Bq/cm^3 of tissue volume by calibration after correction for decay and attenuation.

Statistics

Data on positron emitter labeling efficiency, particle size, and zeta potential of LEH by SophT method were displayed as mean ± standard deviation. Changes in LEH properties by labeling were determined by paired Student t-test.

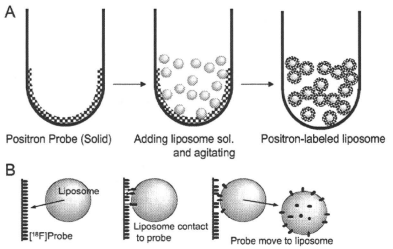

FIG. 2. The overview of positron emitter labeling procedure by SophT method. (A) Solvent-free positron emitter probe ([^{18}F]-probe) was prepared by semiautomated synthesizing system. Preformulated LEH was added to the tube and agitated gently. The solution was transferred and centrifuged to remove unbound probe. (B) During the agitation, the ^{18}F-probe is transited to lipid phase of LEH directly.

RESULTS

Labeling of LEH by SophT method

The solid form of positron emitter labeled probe (Fig. 1) in a glass vial was prepared by semiautomated system (Fig. 2A). Supplied LEH (TRM-645) was added to the vial with [^{18}F]SteP2 and agitated to transfer the probe to the lipid bilayer surface of LEH (Fig. 2B). Incorporation of [^{18}F]SteP2 into lipid assemblies by SophT method was performed around the phase transition temperature of its lipid components to achieve high labeling efficiency. To protect the hemoglobin in LEH from the functional loss by heating, the labeling temperature was set at around 37°C. The labeling efficiency of LEH was 46.4 ± 4.8%, and its radioactivity was high enough for positron imaging by the small animal PET system. The operation of SophT method did not affect the biochemical properties of LEH, such as the particle sizes (PRE 216.5 ± 7.9 nm vs. POST 211.0 ± 1.8 nm, P = not significant [NS]) and zeta potentials (PRE −7.52 ± 0.22 mV vs. POST −7.40 ± 0.66 mV, P = NS).

Distribution of LEH in the ischemic region

At first, the CBF in the ischemic region of the brain was examined by [^{15}O]H_2O PET; [^{15}O]H_2O was injected via tail vein and PET imaging was acquired for 2 min. The imaging of [^{15}O]H_2O distribution (Fig. 3A) indicated the decrease of CBF in the left middle brain, downstream of the MCA occluded by PIT. After the confirmation of suppressed CBF in the left hemisphere, [^{18}F]-labeled LEH was administrated via tail vein. The imaging of [^{18}F]-labeled LEH was acquired for 60 min, and images were integrated every 5 min (Fig 3B). In the early phase, there was little signal of [^{18}F]-labeled LEH in the ischemic area determined by the immediately preceding [^{15}O]H_2O PET images (Fig. 3A). During the 60-min scan, the radioactivity of [^{18}F]-labeled LEH was gradually increased in the cerebral cortex, but there was no detectable signal in the ischemic core, which corresponds to basal ganglia.

DISCUSSION

Real-time visualization of liposomal nanocapsule, including LEH, is desirable to clarify its pharmacodynamics and mechanism of action. Liposomal nanocapsules would be labeled with [^{18}F]fluorodeoxyglucose (11,12) or water-insoluble [^{18}F]fluorodipalmitin (13), although the labeling of liposome with these radioactive probes usually requires modification or reconstitution of its membrane. Furthermore, liposomal drugs are the products of multiple steps (4,5), requiring much longer process than the half-lives of commonly used positron emitter nuclei, ^{11}C (20 min) or ^{18}F (108 min). Thus, labeling preformulated DDS drugs or substituting components of liposome is impractical. In the present study, we tested 1-[^{18}F]fluoro-3,6-dioxatetracosane (Fig. 1) and found a high labeling efficiency without changing the physiological or electrical properties of LEH. A small animal PET system with a high spatial resolution made possible in vivo imaging of [^{18}F]-labeled-LEH in a rat brain ischemia model. The moment-to-moment distribution of LEH was clearly visualized in the ischemic area confirmed by the [^{15}O]H_2O PET. These findings suggest that [^{18}F]SteP2 is a promising PET probe for imaging of LEH in vivo in small animals used with a PET system with a high resolution and signal to noise ratio (10).

We recently reported that the administration of LEH significantly reduces the size of cerebral infarction (14) in PIT model in the rat as well as in the primate (15); the cerebral cortex was preferentially protected than basal ganglia. The disparate effects prompted the current study to evaluate a hypothesis that LEH improve microcirculation and O_2 delivery (14,15). The current observation that [^{18}F]-labeled LEH signal gradually increased in the cortex but not in basal ganglia during the initial 60 min after administration are compatible with the hypothesis. The histological results (14,15) were also in accordance with the distribution of [^{18}F]-labeled LEH. These results may lead to a clue to the mechanism of action of

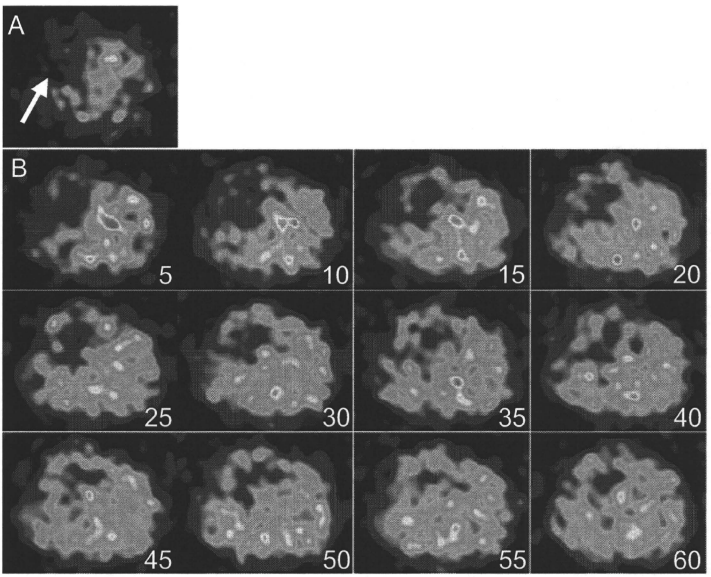

FIG. 3. PET imaging of $[^{15}O]H_2O$ and $[^{18}F]$SteP2 distribution in an ischemic rat brain. (A) $[^{15}O]H_2O$ was administered via tail vein. The distribution of $[^{15}O]H_2O$ was scanned by small animal PET system, Clairvivo. The original data were reconstructed and 2-min data were integrated to an image. The arrow presented the ischemic region in the left brain of the PIT thrombosis of MCA model rat. (B) LEH labeled with $[^{18}F]$SteP2 was administered via a tail vein 20 min after the $[^{15}O]H_2O$ PET scanning. The data were acquired for 60 min and integrated every 5 min. Although the figure shows the typical images obtained in one experiment, another three separate experiments with the same procedure were performed and obtained similar results.

LEH in the focal organ ischemia and/or infarction. Awasthi and coworkers previously reported that LEH had the significant oxygen-carrying and delivery capacity, and improved hypovolemia-induced decrease in cerebral metabolic rate of oxygen by the use of $[^{15}O]$-PET (16). The results obtained in this study are consistent with their results.

Stability of $[^{18}F]$SteP2 in LEH in the bloodstream is an important issue. We previously examined the stability of $[^{18}F]$SteP2 in the liposomes composed of distearoylphosphatidylcholine and choresterol, of which characteristics are similar to that of LEH composed of hydrogenated phosphatidylcholine, cholesterol, and stearic acid. Our results indicated that the transfer of $[^{18}F]$SteP2 to serum components, including lipoprotein, was less than 10% after incubation in 50% fetal bovine serum for 30 min at 37°C (8). Therefore, PET images obtained in this study may reflect LEH biodistribution.

CONCLUSIONS

Labeling LEH with $[^{18}F]$SteP2 provided a high labeling efficiency in a short period of time, and allowed the real-time visualization of LEH in the rat vivo by an enhanced PET system. This labeling-and-detection PET system may make experimental evaluation of new drugs in small animals possible and easier than the current testing on larger animals or humans using regular PET system.

Acknowledgments: This study was supported by a grant from Central Shizuoka Cooperation of Innovative Technology and Advanced Research in Evolution Area (City Area) of the Ministry of Education, Culture, Sports, Science, and Technology (MEXT), COE Program in the 21st Century of MEXT, and CREST of Japan Science and Technology Agency (JST), Saitama, Japan.

REFERENCES

1. Adler-Moore J. AmBisome targeting to fungal infections. *Bone Marrow Transplant* 1994;14(Suppl. 5):S3–7.
2. Minko T, Pakunlu RI, Wang Y, Khandare JJ, Saad M. New generation of liposomal drugs for cancer. *Anticancer Agents Med Chem* 2006;6:537–52.
3. Pedroso de Lima MC, Neves S, Filipe A, Duzgunes N, Simoes S. Cationic liposomes for gene delivery: from biophysics to biological applications. *Curr Med Chem* 2003;10:1221–31.
4. Sakai H, Sou K, Horinouchi H, Kobayashi K, Tsuchida E. Review of hemoglobin-vesicles as artificial oxygen carriers. *Artif Organs* 2009;33:139–45.
5. Kaneda S, Ishizuka T, Goto H, Kimura T, Inaba K, Kasukawa H. Liposome-encapsulated hemoglobin, TRM-645: current status of the development and important issues for clinical application. *Artif Organs* 2009;33:146–52.
6. Buchan P. Smarter candidate selection—utilizing microdosing in exploratory clinical studies. *Ernst Schering Res Found Workshop* 2007;59:7–27.
7. Bergstrom M, Grahnen A, Langstrom B. Positron emission tomography microdosing: a new concept with application in tracer and early clinical drug development. *Eur J Clin Pharmacol* 2003;59:357–66.
8. Urakami T, Akai S, Katayama Y, Harada N, Tsukada H, Oku N. Novel amphiphilic probes for [^{18}F]-radiolabeling preformed liposomes, and determination of liposomal trafficking by positron emission tomography. *J Med Chem* 2007;50:6454–7.
9. Takamatsu H, Kondo K, Ikeda Y, Umemura K. Neuroprotective effects depend on the model of focal ischemia following middle cerebral artery occlusion. *Eur J Pharmacol* 1998;362: 137–42.
10. Mizuta T, Kitamura K, Iwata H, et al. Performance evaluation of a high-sensitivity large-aperture small animal PET scanner: clairvivo PET. *Ann Nucl Med* 2008;22:447–55.
11. Oku N, Tokudome Y, Tsukada H, Kosugi T, Namba Y, Okada S. In vivo trafficking of long-circulating liposomes in tumour-bearing mice determined by positron emission tomography. *Biopharm Drug Dispos* 1996;17:435–41.
12. Oku N, Tokudome Y, Tsukada H, Okada S. Real-time analysis of liposomal trafficking in tumor-bearing mice by use of positron emission tomography. *Biochim Biophys Acta* 1995; 1238:86–90.
13. Marik J, Tartis MS, Zhang H, et al. Long-circulating liposomes radiolabeled with [18F]fluorodipalmitin ([^{18}F]FDP). *Nucl Med Biol* 2007;34:165–71.
14. Kawaguchi AT, Fukumoto D, Haida M, Ogata Y, Yamano M, Tsukada H. Liposome-encapsulated hemoglobin reduces the size of cerebral infarction in the rat: evaluation with photochemically induced thrombosis of the middle cerebral artery. *Stroke* 2007;38:1626–32.
15. Kawaguchi AT, Haida M, Yamano M, Ogata Y, Tsukada H. O_2 affinity, dose-response relationship, and long-term effect of artificial O_2 carrier after brain ischemia and reperfusion in the primate [Abstract]. *Stroke* 2007;38:599.
16. Awasthi V, Yee SH, Jerabek P, Goins B, Phillips WT. Cerebral oxygen delivery by liposome-encapsulated hemoglobin: a positron-emission tomographic evaluation in a rat model of hemorrhagic shock. *J Appl Physiol* 2007;103:28–38.

International Journal of Pharmaceutics 362 (2008) 197–200

Contents lists available at ScienceDirect

International Journal of Pharmaceutics

journal homepage: www.elsevier.com/locate/ijpharm

Note

Particle size-dependent triggering of accelerated blood clearance phenomenon

Hiroyuki Koide[a], Tomohiro Asai[a], Kentaro Hatanaka[a], Takeo Urakami[a], Takayuki Ishii[a], Eriya Kenjo[a], Masamichi Nishihara[b], Masayuki Yokoyama[b], Tatsuhiro Ishida[c], Hiroshi Kiwada[c], Naoto Oku[a,*]

[a] *Department of Medical Biochemistry and Global COE Program, Graduate School of Pharmaceutical Sciences, University of Shizuoka, 52-1 Yada, Suruga-ku, Shizuoka 422-8526, Japan*
[b] *Kanagawa Academy of Science and Technology, KSP East 404, Sakado 3-2-1, Takatsu-ku, Kawasaki, Kanagawa 213-0012, Japan*
[c] *Department of Pharmacokinetics and Biopharmaceutics, Institute of Health Biosciences, The University of Tokushima, 1-78-1 Sho-machi, Tokushima 770-8505, Japan*

ARTICLE INFO

Article history:
Received 22 April 2008
Received in revised form 29 May 2008
Accepted 4 June 2008
Available online 7 June 2008

Keywords:
Polyethylene glycol
Liposomes
Accelerated blood clearance
Polymeric micelles
Nanocarriers

ABSTRACT

A repeat-injection of polyethylene glycol-modified liposomes (PEGylated liposomes) causes a rapid clearance of them from the blood circulation in certain cases that is referred to as the accelerated blood clearance (ABC) phenomenon. In the present study, we examined whether polymeric micelles trigger ABC phenomenon or not. As a preconditioning treatment, polymeric micelles (9.7, 31.5, or 50.2 nm in diameter) or PEGylated liposomes (119, 261 or 795 nm) were preadministered into BALB/c mice. Three days after the preadministration [^{3}H]-labeled PEGylated liposomes (127 nm) as a test dose were administered into the mice to determine the biodistribution of PEGylated liposomes. At 24 h after the test dose was given, accelerated clearance of PEGylated liposomes from the bloodstream and significant accumulation in the liver was observed in the mice preadministered with 50.2–795 nm nanoassemblies (PEGylated liposomes or polymeric micelles). In contrast, such phenomenon was not observed with 9.7–31.5 nm polymeric micelles. The enhanced blood clearance and hepatic uptake of the test dose (ABC phenomenon) were related to the size of triggering nanoassemblies. Our study provides important information for developing both drug and gene delivery systems by means of nanocarriers.

1. Introduction

PEGylated liposomes possessing a long-circulating characteristic have been widely used for delivery systems of both drugs and genes. PEG provides a steric barrier to nanocarriers for avoiding interaction with plasma proteins including opsonins and the cells of mononuclear phagocyte system (MPS) (Allen and Hansen, 1991; Sakakibara et al., 1996; Lasic, 1996). However, our recent reports demonstrated that the intravenous injection of PEGylated liposomes might significantly alter a pharmacokinetic behavior of them injected thereafter (Ishida et al., 2006a,c; Wang et al., 2007). A repeat-injection of PEGylated liposomes causes a rapid clearance of them from the blood circulation in certain cases. This phenomenon, referred to as the accelerated blood clearance (ABC) phenomenon, is considered to be related with anti-PEG IgM secretion from splenic B cells (Ishida et al., 2006a,c). Anti-PEG IgM, produced in response to an injected dose of PEGylated liposomes, selectively binds to them injected secondary (Wang et al., 2007).

However, the immune response against polymeric micelles was not known at all. Polymeric micelles are formed from block copolymers typically consisting of hydrophilic and hydrophobic polymer blocks (Kwon and Kataoka, 1995). They are of particular interest as a drug carrier because of their small particle sizes, efficiency in entrapping a satisfactory amount of hydrophobic drugs within the inner core, stability in the circulation, and their ability of sustained release of the drugs. Polymeric micelles were also considered as a less immune response carrier (Yokoyama et al., 1991; Gaucher et al., 2005).

In this study, we examined whether the preadministration of polymeric micelles possessing PEG chains alters the biodistribution of PEGylated liposomes or not. Moreover, we investigated the

Abbreviations: ABC phenomenon, accelerated blood clearance phenomenon; [^{3}H]-CHE, [^{3}H] cholesterylhexadecyl ether; MPEG-DSPE, 1,2-distearoyl-*sn*-glycero-3-phosphoethanolamine-*n*-[methoxy(polyethylene glycol)-2000]; MPS, mononuclear phagocyte system; PEG-PBLA, poly(ethylene glycol)-*b*-poly(β-benzyl L-aspartate); PEGylated liposomes, polyethylene glycol-modified liposomes.

* Corresponding author. Tel.: +81 54 264 5701; fax: +81 54 264 5705.
E-mail address: oku@u-shizuoka-ken.ac.jp (N. Oku).

0378-5173/$ – see front matter © 2008 Elsevier B.V. All rights reserved.
doi:10.1016/j.ijpharm.2008.06.004

particle size-dependency for triggering the phenomenon by use of PEGylated liposomes and polymeric micelles.

2. Materials and methods

2.1. Materials

Dipalmitoylphosphatidylcholine (DPPC), cholesterol and 1,2-distearoyl-*sn*-glycero-3-phosphoethanolamine-*n*-[methoxy(polyethylene glycol)-2000](MPEG-DSPE) were kindly gifted from Nippon Fine Chemical Co., Ltd. (Takasago, Hyogo, Japan). [^{3}H]cholesterylhexadecyl ether ([^{3}H]-CHE) was purchased from Amersham Pharmacia (Buckinghamshire, UK). All other reagents were analytical grade.

2.2. Animal

Five-week-old male BALB/c mice were purchased from Japan SLC Inc. (Shizuoka, Japan). The animals were cared for according to the animal facility guidelines of the University of Shizuoka. All animal experiments were approved by the Animal and Ethics Review Committee of the University of Shizuoka.

2.3. Preparation of polymeric micelles

Three block copolymers were used for polymeric micelle preparations. Their structures and compositions are summarized in Table 1. Poly (ethylene glycol)-*b*-poly(β-benzyl L-aspartate) (PEG-PBLA) was synthesized by polymerization of β-benzyl L-aspartate *N*-carboxy anhydride from an amino terminal of α-methyl-ω-aminopoly(oxyethylene), as reported previously (Yokoyama et al., 1992). Two partially esterified block copolymers, PEG-P(Asp(pentyl)) and PEG-P(Asp(nonyl)), were prepared by esterification of PEG-*b*-poly(aspartic acid) block copolymer by a reported method (Yamamoto et al., 2007). In brief, aspartic acid residues of PEG-*b*-poly(aspartic acid) block copolymer was activated with 1,8-diazabicyclo[5,4,0]7-undecene, followed by reaction with corresponding alkyl bromides, pentyl bromide and nonyl bromide.

Polymeric micelles were prepared from these three block copolymers by a dialysis method (Yamamoto et al., 2007). Block copolymers were dissolved in DMF at a concentration of 7.5 mg/ml. These polymer solutions were dialyzed against distilled water by the use of a dialysis membrane (Spectra/Por 6, molecular weight cut-off: 1000, Spectrum Japan, Tokyo, Japan). After overnight dialysis, the micelle solutions were concentrated by ultrafiltration (Millipore ultrafiltration membrane PBHK, molecular weight cut-off: 100,000, Nihon Millipore, Tokyo, Japan). By dynamic light scattering, weight-averaged diameters of the obtained polymeric micelles were found to be 50.2, 31.5, and 9.7 nm for PEG-PBLA, PEG-P(Asp(pentyl)), and PEG-P(Asp(nonyl)), respectively.

2.4. Preparation of PEGylated liposomes

PEGylated liposomes composed of DPPC and cholesterol with MPEG-DSPE (10:5:1 as molar ratio) were prepared as described previously (Maeda et al., 2004). In brief, lipids dissolved in chloroform were evaporated to form thin lipid film. Then liposomes were formed by hydration with 10 mM phosphate-buffered 0.3 M sucrose solution (pH 7.4). Then liposomes were sized by five times extrusion through a polycarbonate membrane filter with 100, 400 or 800 nm pores (Nucleopore, Maidstone, UK). For a biodistribution study, a trace amount of [^{3}H]-CHE (74 kBq/mouse) was added to the initial chloroform solution. Particle size of PEGylated liposomes diluted with PBS, pH 7.4, was measured by dynamic light scattering.

2.5. Biodistribution of PEGylated liposomes

Mice were received intravenous injection of polymeric micelles (2.9 mg/kg), PEGylated liposomes (2.0 μmol phospholipids/kg, 2.4 mg total lipids/kg) or phosphate-buffered sucrose. At three days later [^{3}H]-labeled test-dose PEGylated liposomes (5.0 μmol phospholipids/kg) were injected into them via a tail vein. Twenty-four hours after the test-dose administration, the mice were sacrificed for the collection of the blood from the carotid artery. Then the blood treated with heparin was centrifugally separated to obtain the plasma. After the blood was withdrawn, the heart, the lung, the liver, the spleen and the kidney were removed and weighed. The radioactivity in plasma and each organ was determined with a liquid scintillation counter (LSC-3100, Aloka, Tokyo, Japan). Distribution data are presented as % dose per wet tissue. The total amount in plasma was calculated based on the average body weight of the mice, where the average plasma volume was assumed to be 4.27% of the body weight based on the data on total blood volume.

2.6. Statistics

Variance in a group was evaluated by the *F*-test, and differences in biodistribution data, by Student's *t*-test.

3. Results and discussion

At first, we used PEGylated liposomes with 119, 261 or 795 nm diameter as a preconditioning dose. Fig. 1 shows the biodistribution of test-dose PEGylated liposomes (127 nm). The amount of the PEGylated liposomes in the plasma was significantly decreased and that in the liver was significantly increased in the mice preadministered with the PEGylated liposomes. ABC phenomenon was caused by all liposomes tested. Fig. 2 shows the biodistribution of test-dose PEGylated liposomes in the mice preadministered with polymeric micelles (9.7, 31.5 or 50.2 nm) at 3 days before. The mice prereceived

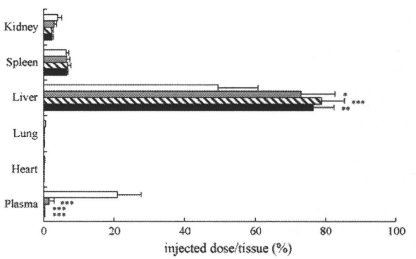

Fig. 1. Biodistribution of test-dose PEGylated liposomes after preadministration of various sized ones. BALB/c mice were intravenously injected with PEGylated liposomes (2.0 μmol phospholipids/kg) with 119, 261 or 795 nm size. Three days later [^{3}H]-labeled test-dose PEGylated liposomes (5.0 μmol phospholipids/kg) were administered via a tail vein. Twenty-four hours later, the mice were sacrificed and the radioactivity in the plasma and each organ was determined ($n = 5$). Data are presented as a percentage of the injected dose per tissue and S.D. Data represent phosphate-buffered sucrose (open bar), 119 nm (gray bar), 261 nm (hatched bar), and 795 nm (closed bar) PEGylated liposomes, respectively. Significant differences against phosphate-buffered sucrose group are shown with asterisks: $^*p < 0.05$; $^{**}p < 0.01$; $^{***}p < 0.001$.

Table 1
Composition of block copolymers

PEG-PBLA

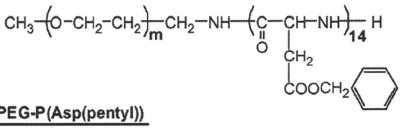

PEG-P(Asp(pentyl))
and PEG-P(Asp(nonyl))

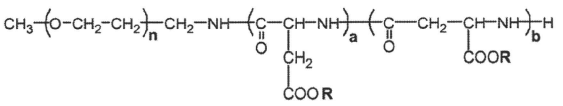

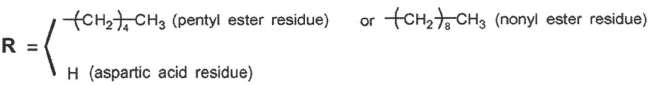

Copolymer	Molecular weight (M.W.)	M.W. of PEG block	Number of Asp units ($a+b$)	Esterification degree (%)[a]	Diameter (nm)[b]
PEG–PBLA	15,000	12,000	14	100	50.2
PEG–P(Asp(pentyl))	9,000	5,000	22	75	31.5
PEG–P(Asp(nonyl))	10,000	5,000	22	72	9.7

[a] Esterification degree (%) = (number of ester residues)/(number of ester residues) + (number of aspartic acid residues) × 100. This degree was determined by ^{1}H NMR measurements.

[b] Weight-weightened average diameter determined by dynamic light scattering.

50.2 nm polymeric micelles showed a significant decrease of test-dose PEGylated liposomes in the plasma and a significant increase in hepatic uptake. However, the preadministration of both 9.7 and 31.5 nm polymeric micelles did not change plasma concentration and hepatic uptake of test-dose PEGylated liposomes. It appears that ABC phenomenon was not caused by preadministration with smaller-sized polymeric micelles (31.5 nm or less), while it was triggered by preadministration with larger-sized polymeric micelles (50.2 nm or more). These results indicate that ABC phenomenon was triggered by preconditioning with not only PEGylated liposomes but also PEG-containing polymeric micelles. Furthermore, the size of nanoassemblies presenting PEG moiety on their surface is one of important factors to induce the ABC phenomenon. In case of large particles, they would be recognized easily by immune cells and activate immune systems, presumably in spleen (Ishida et al., 2006b). By contrast, small particles might avoid the recognition by immune cells. In the point of the molecular weight of PEG moiety, we previously reported that elongation of PEG chain length did not show any difference for inducing ABC phenomenon (Ishida et al., 2005). Consequently, the larger particles may produce anti-PEG IgM (Wang et al., 2007) that triggers enhanced blood clearance and hepatic uptake of test-dose PEGylated liposomes, although further investigation should be required to prove this assumption.

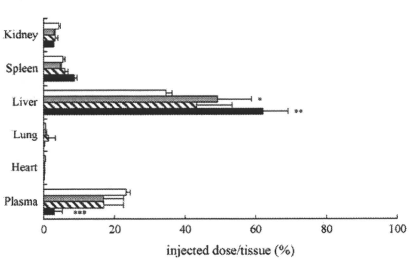

Fig. 2. Biodistribution of test-dose PEGylated liposomes after preadministration of various size polymeric micelles. BALB/c mice were intravenously injected with polymeric micelles (2.9 mg/kg) with 9.7, 31.5 or 50.2 nm size. Three days later [^{3}H]-labeled PEGylated test-dose liposomes (5.0 μmol phospholipids/kg) were administered via a tail vein. Twenty-four hours later, the mice were sacrificed and the radioactivity in the plasma and each organ was determined ($n=5$). Data are presented as a percentage of the injected dose per tissue and S.D. Data represent phosphate-buffered sucrose (open bar), 9.7 nm (gray bar), 31.5 nm (hatched bar), and 50.2 nm (closed bar) polymeric micelles, respectively. Significant differences against phosphate-buffered sucrose group are shown with asterisks: *$p<0.05$; **$p<0.01$; ***$p<0.001$.

4. Conclusions

This study is the first report to demonstrate that the preconditioning with polymeric micelles sized at around 50 nm, which are most widely used to deliver anti-cancer drug, causes the ABC phenomenon. Furthermore, it is clarified that the size of nanoassemblies is one of important factors for ABC phenomenon. Since nanocarriers are now progressing in the field of DDS, this study points out the important information about unexpected immune reactions against nanocarriers.

References

Allen, T.M., Hansen, C.B., 1991. Pharmacokinetics of stealth versus conventional liposomes: effect of dose. Biochim. Biophys. Acta 1068, 133–141.

Gaucher, G., Dufresne, M.H., Sant, V.P., Kang, N., Maysinger, D., Leroux, J.C., 2005. Block copolymer micelles: preparation, characterization and application in drug delivery. J. Control. Release 109, 169–188.

Ishida, T., Harada, M., Wang, X.Y., Ichihara, M., Irimura, K., Kiwada, H., 2005. Accelerated blood clearance of PEGylated liposomes following preceding liposome injection: effects of lipid dose and PEG surface-density and chain length of the first-dose liposomes. J. Control. Release 105, 305–317.

Ishida, T., Atobe, K., Wang, X., Kiwada, H., 2006a. Accelerated blood clearance of PEGylated liposomes upon repeated injections: effect of doxorubicin encapsulation and high-dose first injection. J. Control. Release 115, 251–258.

Ishida, T., Ichihara, M., Wang, X., Kiwada, H., 2006b. Spleen plays an important role in the induction of accelerated blood clearance of PEGylated liposomes. J. Control. Release 115, 243–250.

Ishida, T., Ichihara, M., Wang, X., Yamamoto, K., Kimura, J., Majima, E., Kiwada, H., 2006c. Injection of PEGylated liposomes in rats elicits PEG specific IgM, which is responsible for rapid elimination of a second dose of PEGylated liposomes. J. Control. Release 112, 15–25.

Kwon, G.S., Kataoka, K., 1995. Block copolymer micelles as long-circulating drug vehicles. Adv. Drug Deliv. Rev. 16, 295–301.

Lasic, D.D., 1996. Doxorubicin in sterically stabilized liposomes. Nature 380, 561–562.

Maeda, N., Takeuchi, Y., Takada, M., Sadzuka, Y., Namba, Y., Oku, N., 2004. Anti-neovascular therapy by use of tumor neovasculature-targeted long-circulating liposome. J. Control. Release 100, 41–52.

Sakakibara, T., Chen, F.A., Kida, H., Kunieda, K., Cuenca, R.E., Martin, F.A., Bankert, R.B., 1996. Doxorubicin encapsulated in sterically stabilized liposomes is superior to free drug or drug-containing conventional liposomes at suppressing growth and metastases of human lung tumor xenografts. Cancer Res. 56, 3743–3746.

Wang, X., Ishida, T., Kiwada, H., 2007. Anti-PEG IgM elicited by injection of liposomes is involved in the enhanced blood clearance of a subsequent dose of PEGylated liposomes. J. Control. Release 119, 236–244.

Yamamoto, T., Yokoyama, M., Opanasopit, P., Hayama, A., Kawano, K., Maitani, Y., 2007. What are determining factors for stable drug incorporation into polymeric micelle carriers? Consideration on physical and chemical characters of the micelle inner core. J. Control. Release 123, 11–18.

Yokoyama, M., Kwon, G.S., Okano, T., Sakurai, Y., Seto, T., Kataoka, K., 1992. Preparation of micelle-forming polymer–drug conjugates. Bioconjugate Chem. 3, 295–301.

Yokoyama, M., Okano, T., Sakurai, Y., Ekimoto, H., Shibazaki, C., Kataoka, K., 1991. Toxicity and antitumor activity against solid tumors of micelle-forming polymeric anticancer drug and its extremely long circulation in blood. Cancer Res. 51, 3229–3236.